

Laser tracker surface measurements of the 8.4 m GMT primary mirror segment

Tom L. Zobrist^a, James H. Burge^{a,b}, Hubert M. Martin^b

^aCollege of Optical Sciences, University of Arizona, Tucson, AZ 85721, USA

^bSteward Observatory, University of Arizona, Tucson, AZ 85721, USA

ABSTRACT

We have developed a metrology system that is capable of measuring rough ground and polished surfaces alike, is nearly independent of the nominal surface shape, and can accommodate surfaces up to 8.4 m in diameter. The system couples a commercial laser tracker with an advanced calibration technique and a system of external references. This system was built to guide loose abrasive grinding and initial polishing of the off-axis primary mirror segments for the Giant Magellan Telescope, and will be used to guide the fabrication of the Large Synoptic Survey Telescope primary and tertiary mirrors as well. The results obtained using this system during the fabrication of the first segment of the Giant Magellan Telescope are presented along with an assessment of the expected system accuracy.

Keywords: telescopes, optical fabrication, optical testing, laser metrology, aspheres

1. INTRODUCTION

This paper details the development of an advanced metrology instrument designed to accurately guide the fabrication of large telescope mirror segments during loose-abrasive grinding. The instrument, referred to as the Laser Tracker Plus system, couples a commercial laser tracker with an advanced calibration technique and a set of external references to mitigate a number of error sources.^{1 2} The Laser Tracker Plus system builds on previous experience of using laser trackers for measuring optical surfaces. The system is further expected to corroborate the optical interferometric test of the polished mirror, in several low-order aberrations. The design, analysis, calibration, and measured performance of the Laser Tracker Plus system will be presented.

This system was designed specifically to guide the loose-abrasive grinding of the Giant Magellan Telescope (GMT) primary mirror segments.³ The GMT design uses seven 8.4 m mirror segments arranged in a close pack structure that produces an $f/0.7$ ellipsoidal parent mirror with an effective aperture of about 25 m.⁴ The central segment is on-axis, while the surrounding six segments are all off-axis. Each of the six identical off-axis segments has a best-fit radius of curvature (RoC) of 38 m, and 14.5 mm of peak to valley aspheric departure.⁵ Figure 1 shows a computer image depicting GMT. New methods and hardware were developed to test GMT because of the off-axis nature of the segment, the very large aspheric departure, and the long RoC. Laser trackers work almost equally well for any surface geometry, making them a good choice for profiling the GMT surface.

A laser tracker is a commercial device that measures the position of a retroreflector in 3 dimensions by using a distance-measuring interferometer and two angular encoders. It is sensitive to sub-micron displacements in the radial direction, and the encoder accuracy is on the order of 1 arcsecond. It is capable of measuring a mirror surface to sub-micron accuracy if the tracker is located at the center of curvature (CoC), so angular errors do not affect the surface measurement, and if rigid-body motion of the mirror and tracker can be controlled during the course of the measurement, typically several minutes to an hour. We have demonstrated this sort of accuracy in measurements of a 1.7 m off-axis mirror.⁶

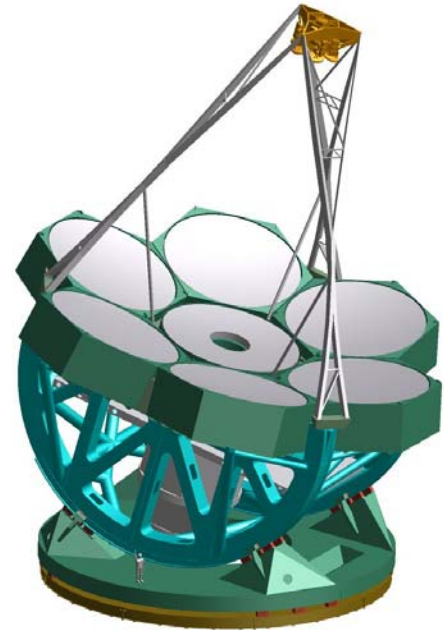


Figure 1: The 25 m $f/0.7$ GMT primary mirror is made of 8.4-m diameter segments.

During loose-abrasive grinding and initial polishing of the GMT segment, the optical surface is periodically measured using the laser tracker mounted 22.3 m above the mirror surface in the test tower. To measure the segment, a sphere-mounted retroreflector (SMR), which is a retroreflecting corner-cube mounted in a small steel sphere with the corner of the cube at the center of the sphere, is moved across the surface and its position is measured by the laser tracker. A set of stability references is used to improve the accuracy of these measurements by compensating for rigid-body motion and refractive index variations. A minimum system accuracy of $2\ \mu\text{m}$ rms over the entire surface of the segment is required in order to guarantee that interference fringes will be resolved when the transition from Laser Tracker Plus to interferometric testing is made. Furthermore, to provide corroboration of the optical interferometric test of the surface, the system must accurately measure low-order aberrations to about $0.5\ \mu\text{m}$ rms surface.

To achieve these accuracies with a laser tracker when testing a large mirror, we have added:

- Stability references that compensate for rigid-body motion and large-scale variations in refractive index, discussed in Section 2, and
- An advanced calibration of the laser tracker is implemented to improve the angular accuracy, discussed in Section 3.

This enhanced system is the Laser Tracker Plus system, shown in Figure 2, which fulfills two important functions:

- It does not require a specular surface, so we can use it to measure the rough surface to guide the generating and loose abrasive grinding operations.
- We can measure low order shape errors in the polished surface to $< 1\ \mu\text{m}$, providing independent corroboration of these components of the mirror shape.

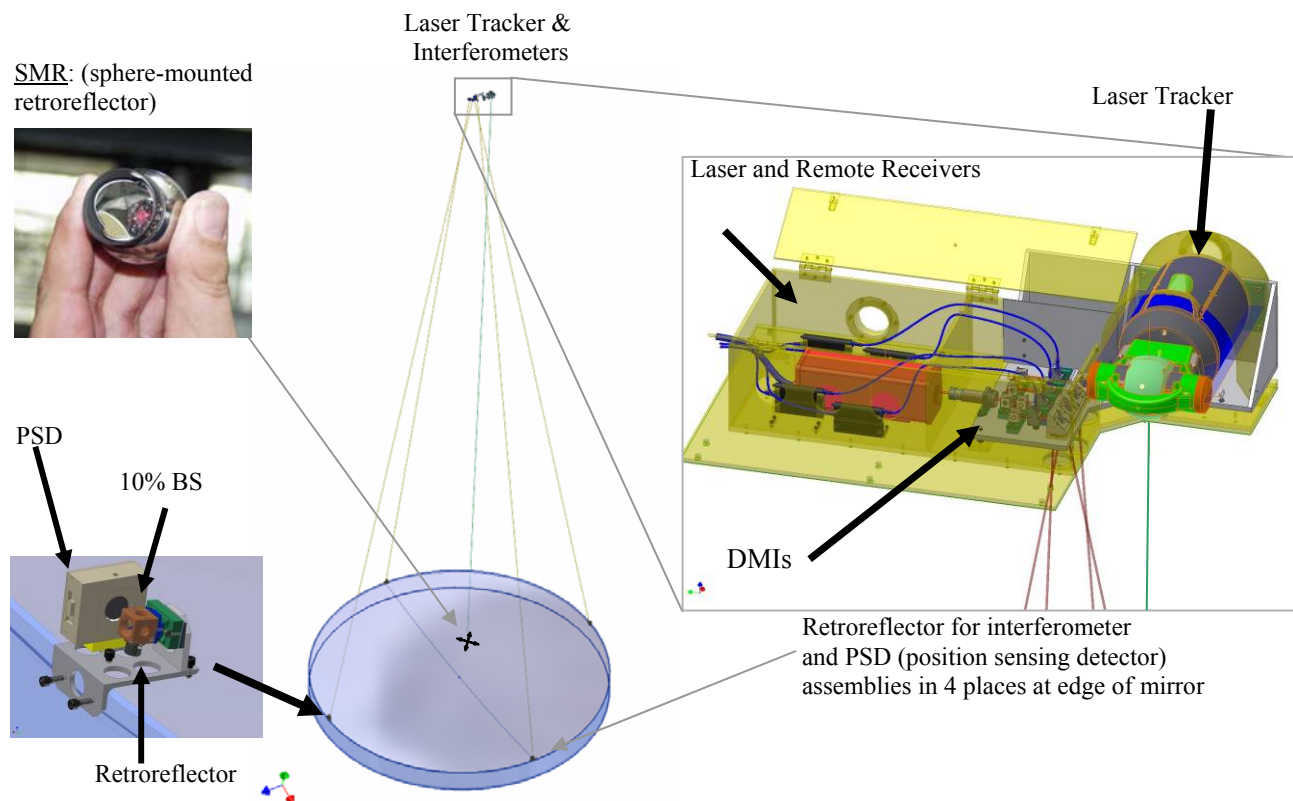


Figure 2: Conceptual drawing of the laser tracker set up for measuring the mirror surface. The laser tracker uses interferometry to measure distance to an SMR (sphere-mounted retroreflector). The tracker runs under servo control to follow the SMR as it is scanned across the surface, combining radial distance with the gimbal angles to make a three-dimensional measurement. Effects due to the combined motion of the air, mirror, and tracker are mitigated by separate real-time measurements of distance and lateral motion using a system of four stability references.

2. LASER TRACKER PLUS SYSTEM DESCRIPTION

The full Laser Tracker Plus system combines three measurement subsystems and a fourth positioning system to accurately measure an optical surface. The three measurement subsystems are a commercial laser tracker, along with four distance measuring interferometers (DMI) and four position sensing detectors (PSD) which together form the external reference system. The positioning system moves the SMR between measurement locations across the mirror surface.

2.1 External reference system

The external reference system is a system of stability references added to enhance the performance of a stand-alone laser tracker by compensating for rigid-body motion and large-scale variations in refractive index, as illustrated in Figure 3. The system includes four stand-alone DMIs, mounted on the same platform with the laser tracker, which monitor fixed retroreflectors at the edge of the mirror. They monitor the changes in the radial path length due to relative motion along the line of sight and changes in optical path length due to index variations. Some of the light from each of the DMIs is deflected to a PSD to monitor the lateral fluctuations of the reference laser beam perpendicular to the line of sight, including the effect of tilt of the laser tracker platform, and lateral motion of the beams due to relative motion of the mirror and laser tracker or index variations. This information is used to correct the laser tracker measurements of points on the mirror surface. The measurements of the reference arms are made simultaneously with the laser tracker measurements.

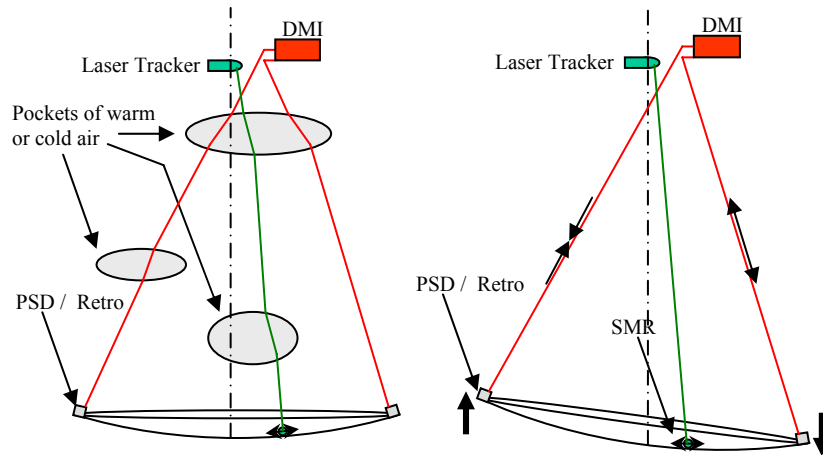


Figure 3: The external reference system is used to compensate for refractive index variations as shown in the figure on the left, and for relative motion between the test instruments and the mirror surface as shown in the figure on the right.

2.2 SMR positioning system

A measurement with the Laser Tracker Plus system consists of ~200 samples with 0.5 m spacing uniformly distributed over the surface. The system includes a mechanism that moves the SMR over the surface of the mirror safely under computer control. This allows mirrors up to 8.4 m diameter to be measured without people being on the mirror or its support platform. It minimizes changing loads that would cause rigid-body motion.

The 1.5 inch SMR is carried by an air puck that has three small flexible rubber air bearings that can glide across a polished surface without scratching. The SMR rests directly on the glass while tracker data are recorded. Air pressure is applied to lift the puck and SMR ~1 mm above the surface while the air bearings remain nearly in contact with the glass. The puck slides to the next position with minimal force, and slowly lowers the SMR to the surface as the air bleeds out. The puck is attached to four strings that control its position, as shown in Figure 4. The strings are controlled by motorized winches, two with position control and two holding constant tension. The winches and associated pulleys are mounted on steel beams about 3 m above floor level (slightly above the mirror surface) where they can be left permanently without interfering with traffic in the lab. Limit switches constrain the range of string positions so they cannot pull the SMR off the mirror or contact the four retroreflector/PSD assemblies at the edge of the mirror.

The SMR follows a pattern programmed into the control computer, pausing at each sample point long enough for the laser tracker and external reference system to make measurements before moving on to the next point. We aim to

control the position to an accuracy of a few cm. The precise sample locations do not matter because the position is measured by the laser tracker.

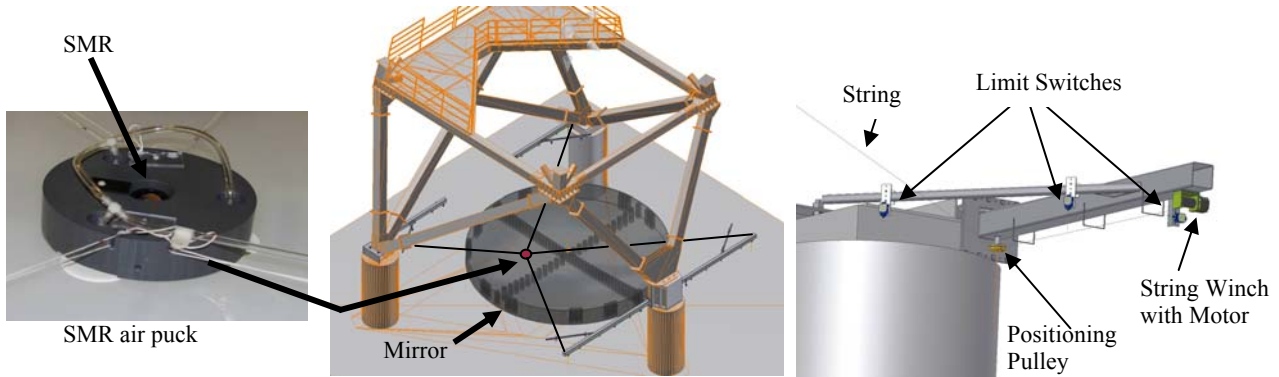


Figure 4: Diagram of the SMR positioning system at the base of the test tower. The gray disk represents the mirror under test, while the small circle at the intersection of the four strings is the location of the SMR puck. A close-up of one of the string control mechanism is shown on the right.

3. CORRELATION RESULTS

A study was conducted using the Laser Tracker Plus system to compare the fluctuations measured by the stability references and the laser tracker, when the references and the SMR are mounted on the floor of the Steward Observatory Mirror Laboratory (SOML) test tower. The references were initially positioned on blocks on the floor so that they were nominally along the same lines of sight that they would be on if they were positioned around the edges of an 8.4 m mirror. A nest with a laser tracker SMR was placed atop the same block that the north surface reference was mounted on. Data were measured for an extended period of time with a 1 s measurement interval, which was decided to be a reasonable time interval for each measurement point and allows the individual measurement points to be averaged to evaluate the effect of integration time.

3.1 Radial correlation

The results of the radial correlation study show that over 5 minute time periods, the fluctuations measured by the laser tracker are about $0.07 \mu\text{m}$ rms, while the fluctuations measured by the DMIs for the same time was $0.2 \mu\text{m}$ rms, indicating that the DMIs are affected by environmental or instrumental noise more than the laser tracker. This means that if everything was stable during a measurement, then we would not want to apply the DMI correction, for that would just couple noise into the laser tracker measurements. However, during a typical GMT surface measurement, a significant amount of rigid-body motion does occur, as can be seen in Figure 5. Figure 6 shows data measured during the correlation study that shows the radial fluctuations measured by the laser tracker and DMIs are well correlated over longer time periods where there is an appreciable amount of motion, probably thermal expansion of the test tower.

To apply the DMI correction, we fit the rigid-body motion to the 4 radial displacements of the reference arms, using the redundant information to check for inconsistencies in the reference data. The correction to the tracker measurement is obtained by taking the best-fit rigid-body displacement and evaluating it at the location of the SMR. Large-scale refractive index variations may look much like

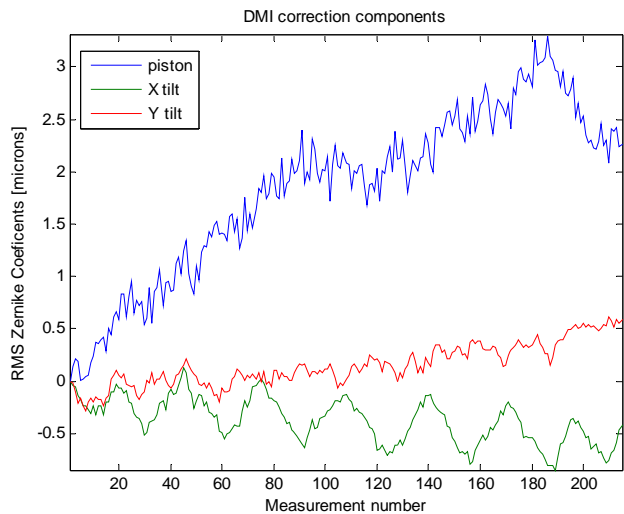


Figure 5: Plots showing the amount of the piston, tip, tilt, and astigmatism measured by the distance measuring interferometer reference system during a typical GMT measurement set.

rigid-body motion and they can be corrected with the same recipe. If the variations are on such a small scale that there is little correlation between the effects at the SMR and the nearest reference arm, there is no point in applying a correction, and the way to improve the measurement is to average over a longer time.

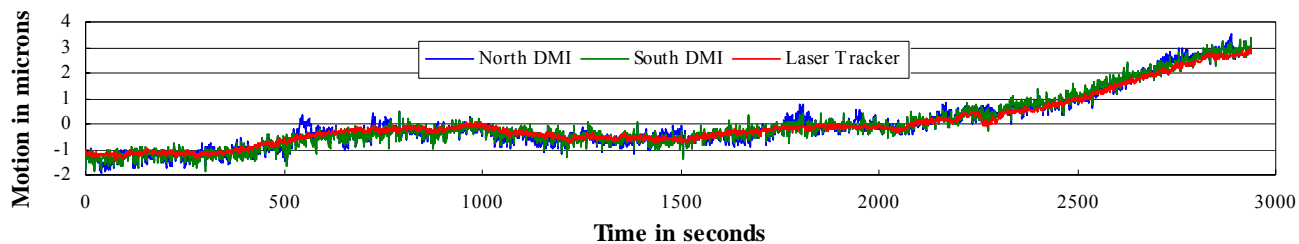


Figure 6: Comparison of radial fluctuations measured by the laser tracker and the north and south DMI references during 1 hour.

3.2 Angular correlation

The results of the angular correlation study show little or no correlation between the laser tracker and the PSD references. Over 5 minute time periods, the fluctuations measured by the laser tracker are about $0.4 \mu\text{rad}$ rms, while the fluctuations measured by the PSDs are $\sim 1.0 \mu\text{rad}$ rms, indicating that the PSDs are affected by environmental or instrumental noise more than the laser tracker. Even over time periods of around 1 hour, the laser tracker fluctuations are only $0.5 \mu\text{rad}$, which indicates that no PSD correction is required. Applying the PSD correction to the laser tracker surface measurements would couple noise into the measurements, so we do not perform a PSD correction to the surface measurements. Figure 7 shows the angular fluctuations measured for the laser tracker during the same hour long data set that generated the radial plot in Figure 6.

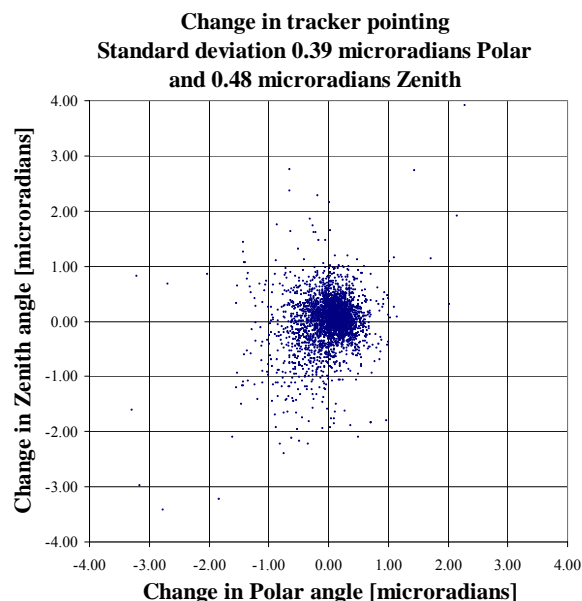


Figure 7: Typical measurement of angular fluctuations experienced by laser tracker over an hour.

4. CUSTOM LASER TRACKER CALIBRATION

To improve the accuracy of the commercial laser tracker, we devised a set of custom calibrations to measure repeatable intrinsic errors in the laser tracker. There are both radial and angular calibrations which determine the repeatable errors in the laser tracker's measurement of radius as a function of angle, and each angle as a function of angle.

4.1 Radial calibration

We calibrate the measurement of radial displacement by measuring a small reference sphere from its center of curvature. The measurement is insensitive to angular errors, allowing a determination of the repeatable portion of the radial error. A 150 mm diameter $f/1.6$ spherical mirror was selected, covering a larger solid angle than the $f/2.6$ cone that an 8.4 m mirror subtends from the tracker. Additionally, the size of the mirror allows it to be installed for *in situ* calibration of the laser tracker while it is mounted in the tower.

The results of the radial calibration indicate that the radial errors in the laser tracker are negligible. Thirty separate measurements of the test mirror were made, showing that the average radial error is less than $1/20 \mu\text{m}$ rms. We fit 45 Zernike polynomials to each measurement. We calculated the mean and standard deviation of each Zernike coefficient, and used them to generate the table and plot in Figure 8. The tilt and power aberrations are due to

displacement of the laser tracker and can be neglected. This leaves the 0 degree astigmatism term to be the largest outlier at 0.03 μm . The operational goal for the Laser Tracker Plus system is 0.25 μm , so any aberration less than 0.05 μm is considered negligible. No correction for radial errors is required.

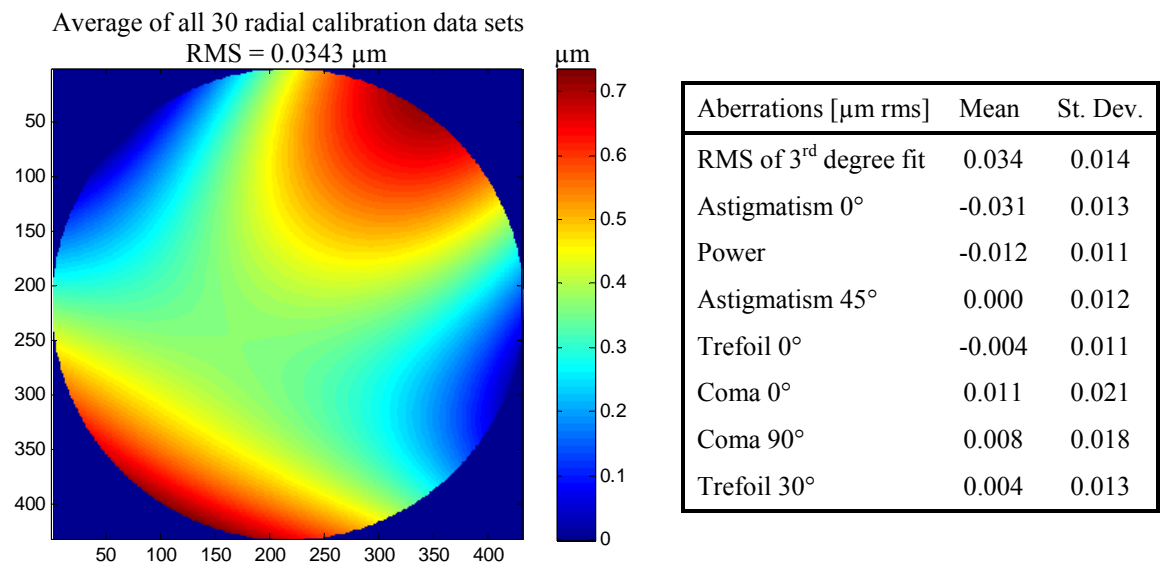


Figure 8: Average surface plot of the Zernike polynomial fit to the residual surface errors from all 30 radial calibration sphere measurements. The mean and standard deviation of all thirty data sets is provided in the table. All aberrations are less than 1/20 $\mu\text{m rms}$, so we can neglect them. Standard deviation is larger for most aberrations than the mean, so value of mean is mostly driven by noise.

4.2 Angular calibration

The 3D accuracy of a laser tracker measurement is limited by the angular component of the measurement. The purpose of the angular calibration is to improve the angular accuracy by performing a custom calibration of one laser tracker with the use of a second laser tracker. The second laser tracker could be replaced by a stand-alone DMI.

The laser tracker in the tower is calibrated by a second laser tracker mounted on the floor, as shown in Figure 9. The tracker in the tower measures horizontal displacement of an SMR with its angular encoders, while the floor-mounted tracker measures the same displacement much more accurately with its DMI. The SMR has a narrow angle of acceptance, so a fixture has been designed that holds three 1.5 inch SMRs in direct contact along a straight line. The two outer balls are aimed upward toward the tracker to be calibrated, while the center ball is aimed horizontally toward the tracker on the floor. By measuring the locations of the two outer balls, the location of the center ball can be calculated.

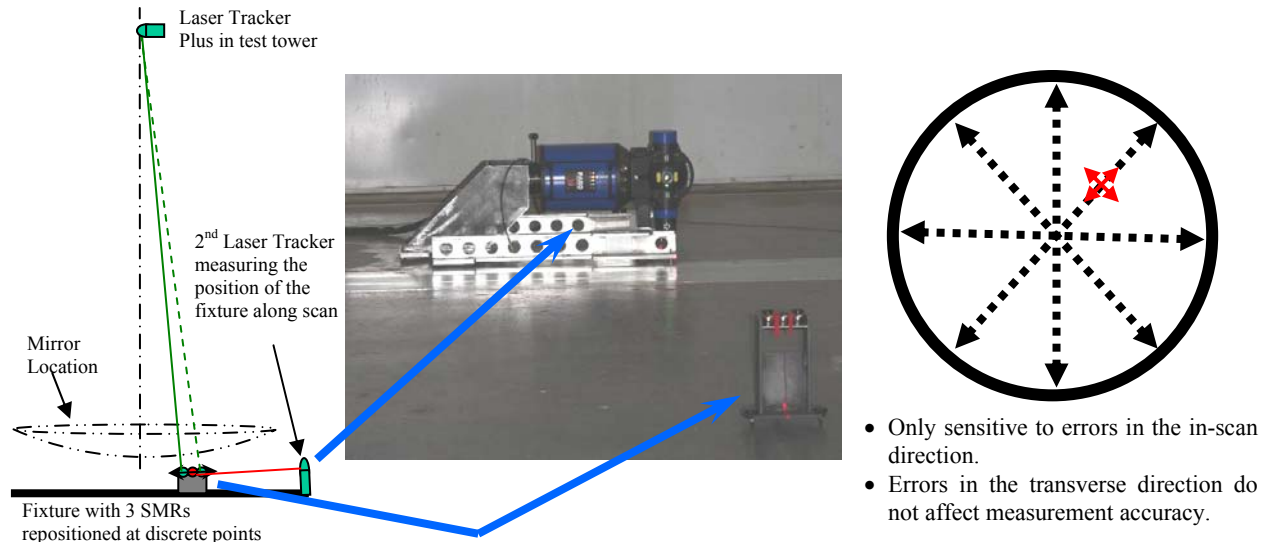


Figure 9: The diagram on the left shows the layout for the angular calibration. The laser tracker at floor measures the fixture location with small angular error compared to the tower tracker. The diagram on the right shows the pattern of multiple scans made to determine the discrepancy between the two trackers, which is used to determine a calibration correction for the angular errors.

Four scan lines were marked on the floor, two of them aligned to the rotation angles of the laser tracker in the tower, while the other two are the 45° lines in between. All four scans cross at the point directly beneath the laser tracker in the tower, where the error is defined to be zero. A 0.5 m measurement spacing was selected along each scan for a total of 21 measurements per scan over a 10 m scan diameter, which is approximately the diameter of the circle subtended by the GMT mirror when projected to the floor. For each scan, the floor laser tracker was set up so its line of sight is aligned to one of these scan lines along the floor. At each measurement position, the laser tracker at floor level measured the location of the center ball in interferometric mode (IFM), which uses a precision DMI to measure the radial displacements. At the same time, the tower tracker measured the location of the outer two outer balls in absolute distance mode, which determines the radial distance by modulating the laser beam. The two outer ball measurements are then averaged together. The assumption is that the laser tracker at the floor measuring in IFM with its DMI has much better accuracy than the tracker in the tower, so any discrepancy between the two sets of measurements is an angular error in the tower tracker. The difference between the two trackers' measured in-scan distance change is the angular error in the laser tracker, shown in Figure 10.

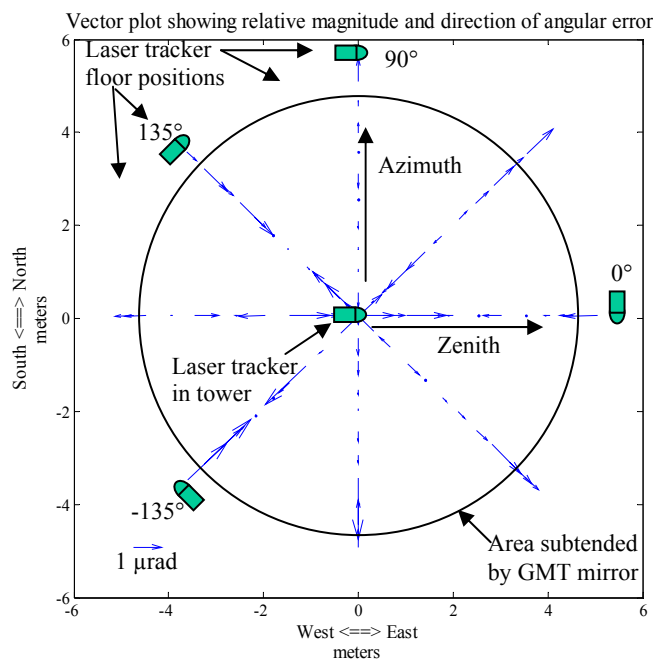


Figure 10: Angular calibration measurement results using four radial scans crossing directly beneath the tower laser tracker to be calibrated. The blue arrows show the direction and relative angular error of the tower tracker.

The results of the angular calibration indicate the angular errors are quite small, less than about 1 μrad rms, but statistically significant and worth correcting. The four scans are fit by polynomials, for instance Zhao's \bar{s} polynomials, to interpolate the angular error across the mirror.⁷ From the polynomials fit, the angular error is computed at each surface measurement location and the angular values measured by the laser tracker are modified to account for the errors. The residual error after correction is reduced to about 0.5 μrad rms, which is consistent with noise in the laser tracker.

5. DATA COLLECTION AND ANALYSIS

The purpose of the measurement is to compare the actual surface of the mirror with the ideal off-axis, near-parabolic surface. The geometric parameters – radius of curvature, off-axis distance, and clocking – are fixed. No fitting is performed to determine the best-fit off-axis surface with varying off-axis distance or radius of curvature. All departures from the ideal surface are treated as errors to be corrected by figuring. Variation of the geometric parameters is only allowed toward the end of the fabrication process, when the figuring is guided by optical measurements, not at the early stages when the laser tracker measurements guide the process.

The laser tracker measurement consists of a number of samples (typically 200–250) on the surface, four geometry reference points that are used to define the off-axis distance and clocking, and the locations of the four retroreflectors of the external reference system. The geometry reference points are near the edge of the segment, at known clocking angles and known distances from both the surface and the outer edge. The segment prescription defines the positions of these references with respect to the optical axis of the parent. Because the four geometry references are measured together with the surface points, the positions of the surface points with respect to the parent axis can be determined. Figure 11 shows the fixture used for measuring the geometry reference marks, along with one of the surface references.

The surface data are collected by moving the SMR puck to predesignated positions across the mirror surface using the SMR positioning system. At each of these locations, the puck comes to rest and the laser tracker and DMIs take simultaneous measurements as fast as they can, and average them over a specific integration time, then the SMR moves on to another position. When an integration time of 1 s is used, it takes about 15 s for the Laser Tracker Plus system to measure then move to the next measurement positions, so the entire surface measurement takes ~1 hour.

Following the measurements, the data are processed to determine the deviation of the actual surface from the ideal surface. The surface points and the reference points are measured initially in the laser tracker's coordinate system. In order to compare the surface data with the ideal surface, all the data are transformed to a parent coordinate system whose origin is at the parent vertex and whose z -axis is the parent axis. The transformation is determined by a least-squares fit to the four geometry reference points, using their measured tracker coordinates and their known parent coordinates. The same transformation is then applied to both the surface data and the surface reference points.

With the surface points transformed to parent coordinates, they can be compared with the ideal surface after applying a compensation for the radius of the SMR. The distance of each point from the surface is then calculated, giving the surface error at each point. These surface errors are displayed in segment coordinates and polynomials are fit to them. The polynomial fit is then used to guide the next grinding run to correct the surface figure errors.

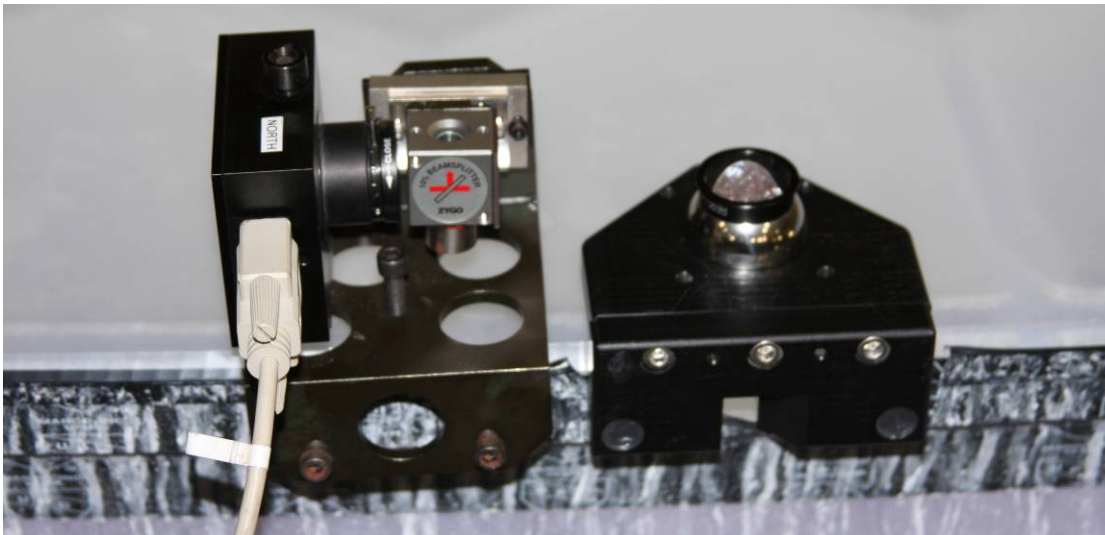


Figure 11: Image of the edge of the GMT mirror segment showing one of the surface references (left) and one of the geometry reference points (an SMR held at a known position, right).

6. EXPERIMENTAL RESULTS

We were able to evaluate the accuracy of the Laser Tracker Plus system by measuring two different mirrors: the large fold sphere (LFS), which was a finished 3.75 m spherical mirror that is now part of the null corrector for the principal optical test of the GMT segment, and the first GMT 8.4 m off-axis segment. At the time of this writing, the GMT principal test is not yet operational, so there are no optical interferometric data to compare with the measurement results from the Laser Tracker Plus system, so a direct comparison cannot be made to evaluate the accuracy of the system as a verification instrument. However, measurements of the LFS were made with the system after the mirror's completion, and the results from those measurements provide evidence that the ultimate accuracy of the Laser tracker Plus system will meet its design requirements.

6.1 Large Fold Sphere Results

The LFS, with a radius of curvature is 25.5 m, was mounted at the base of the 28 m test tower and the Laser Tracker Plus system was in its standard position near the top of the tower, about 22 m above the mirror. At the time of this measurement, the SMR positioning system was not installed, so the SMR was attached to a wooden wand and moved manually from point to point on the mirror surface. We took 93 samples over a 1.5 hour period, averaging the laser tracker, DMIs and PSDs over 10 s for each sample. The laser tracker data were processed by fitting a spherical surface. For each sample we applied the DMI correction by fitting a plane to the 4 DMI displacements (projected to the vertical direction), and evaluating the plane at the lateral position of the SMR (as measured by the laser tracker). Examination of the reference DMI data indicates rigid-body motion of 10 μm peak-to-valley piston and 6 μm p-v tilt during the measurement, and 0.8 μm p-v deviation from the best-fit plane. This deviation may be due to temperature gradients or some kind of drift in the reference DMI system. The DMIs' deviation from a plane was not used as part of the correction of laser tracker data. Figure 12 shows the deviation from the best-fit sphere, before and after applying corrections based on the reference DMIs. The rms deviation is 1.4 μm with no DMI correction, and 0.75 μm after the DMI correction. An optical interferometer measurement was made at about the same time as the Laser Tracker Plus measurement, showing that the mirror surface has about 50 nm rms astigmatism (which will be corrected in operation, along with other low-order aberrations, by the adjustable support) and 40 nm rms in other figure error. The 0.75 μm deviation of the corrected tracker data reflects the accuracy of the Laser Tracker Plus system in this geometry, which is a favorable geometry with almost normal incidence.

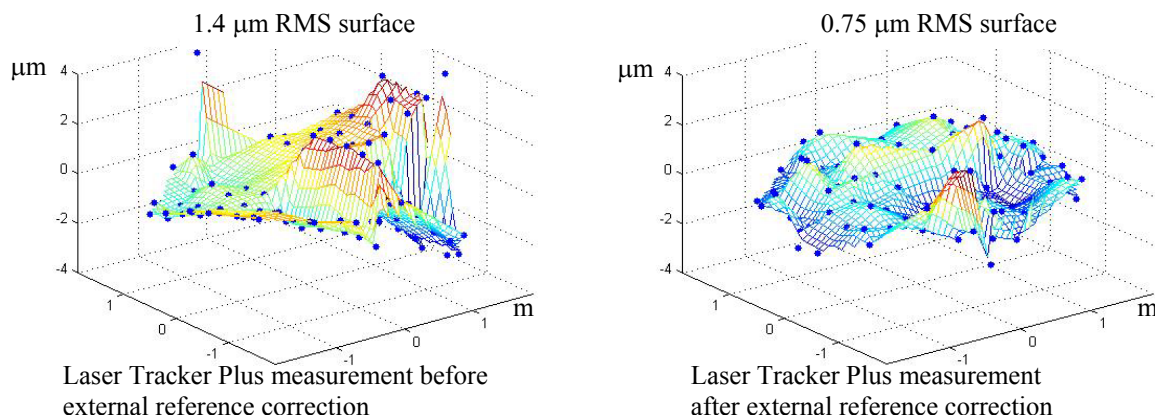


Figure 12: Measurements of a 3.75 m spherical mirror surface with the laser tracker only on the left, and the corrected plot after applying the data from the external reference system. The plots show the departure from the best-fit sphere, in microns.

6.2 GMT Segment 1 results

The Laser Tracker Plus system was used to guide the loose-abrasive grinding of GMT, starting with the first set of measurement in July 2008 and ending in June 2009. Figure 13 shows the GMT mirror under the SOML test tower setup for a Laser Tracker Plus measurement. All four external references are set up around the circumference of the mirror and aligned to the DMI laser beams shining down from the Laser Tracker Plus instrument platform at the top of the tower (not visible in the picture). The air puck is visible on the mirror surface, and with close inspection, the air hose and the strings can be seen leading back to the SMR positioning system.

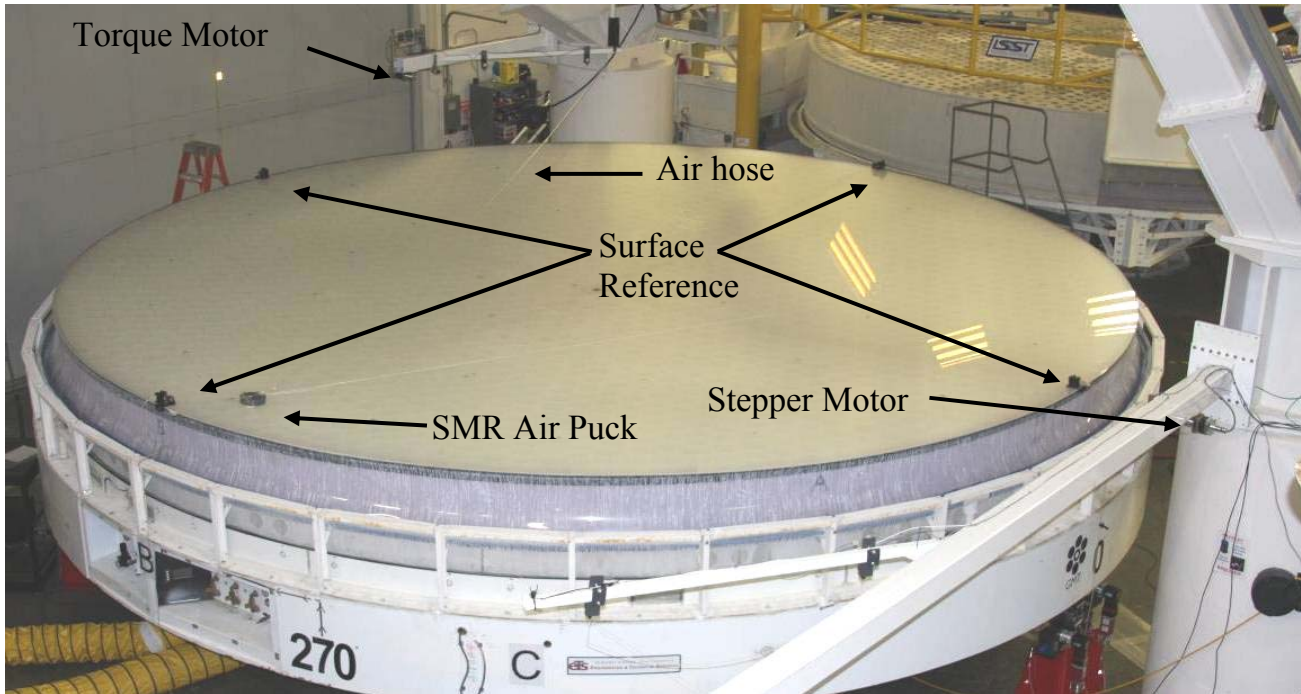


Figure 13: Testing of the 8.4 m GMT mirror segment with the Laser Tracker Plus system. The four surface references are visible at the four compass points around the mirror. The SMR air puck and several components of the SMR positioning system are visible in the picture.

A typical Laser Tracker Plus measurement of the surface consisted of about 200 samples with 0.5 m spacing. The DMI data were used to correct the laser tracker data for rigid-body motion between the mirror and the instruments in the tower during the measurement. The distance of each point from the surface is then calculated, giving the surface error at each point. These surface errors are displayed in segment coordinates and polynomials are fit to them. The coefficients of the polynomial fit are then used to guide the next grinding run to correct the surface figure errors.

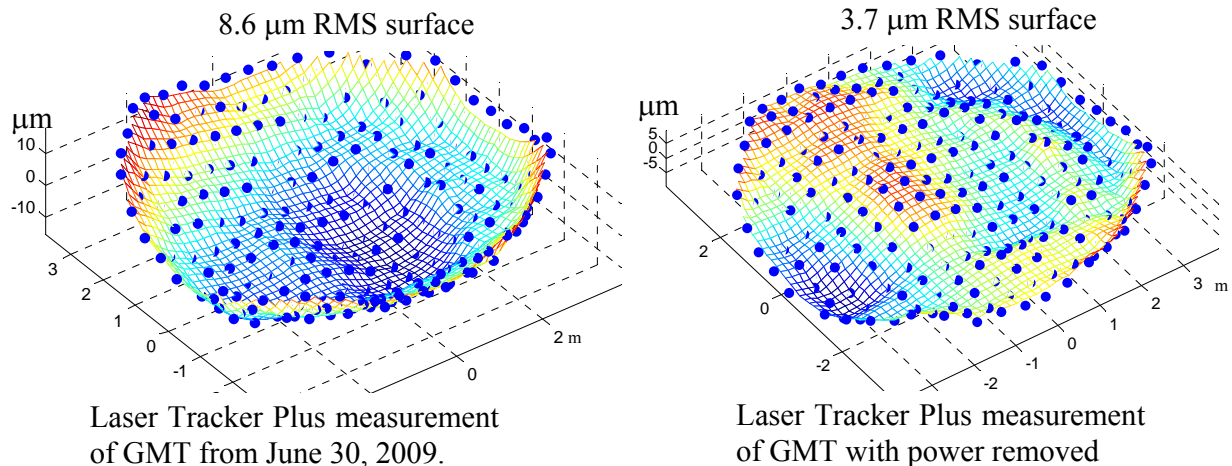


Figure 14: Measurements of the first GMT off-axis mirror segment with the Laser Tracker Plus system at the end of loose-abrasive grinding. The plot on the left show the departure from the ideal surface, in microns, with only piston, tip and tilt removed, while the one on the right also has power removed.

6.3 Test of System Accuracy

Comparison of Laser Tracker Plus measurement data to interferometric measurements made with the GMT principal test will ultimately determine the final system accuracy; however, the answer to that test will have to wait a

while longer. For now, the LFS measurements will be used in lieu of GMT optical data. At the time of the measurements of the LFS, it was a finished optic. The errors in the surface figure were considerably smaller than the measurement resolution of the Laser Tracker Plus system, so for all practical purposes, the surface was perfect. The measurement results presented in Figure 12 show that after applying the DMI reference correction, the residual rms error is only 0.75 μm , and the p-v is less than 4 μm .

Based on the LFS measurement results, the Laser Tracker Plus system is capable of measuring an optical surface with an accuracy down to 0.75 μm . A caveat must be made though, because the RoC of the LFS is 25.5 m, and it was positioned approximately 22 m below the Laser Tracker Plus system, so the laser tracker head was very close to the center of curvature of the LFS, making the measurements less sensitive to angular errors. The sensitivity of the surface measurements to angular errors is 0.24 $\mu\text{m}/\mu\text{rad}$ at the edge of the mirror. Combining this with the laser tracker's angular measurement accuracy of 0.5 μrad rms results in a potential surface error of only 0.12 μm at the edge. The GMT segment is about six times more sensitive to angular errors.

One common way of assessing a measuring system's accuracy is to rotate the part being measured with respect to the measurement instrument. This was done with the GMT mirror to test for systematic errors in the Laser Tracker Plus measurements. Table 1 shows the coefficients from the Zernike polynomial fit for two typical GMT figure measurements made with the Laser Tracker Plus system with the mirror rotated 90° between measurements. The values listed in Table 1 show that the low-order aberrations are around 0.5 μm rms or less. This indicates there are no large intrinsic errors in the system, which provides confidence that the system will meet its verification design goals when the time comes.

Table 1: Comparison of two typical GMT figure measurements made with the Laser Tracker Plus system with the mirror rotated 90° between measurements.

| 0° microns | 90° microns | Average microns | Difference microns | Aberrations rms surface |
|---------------|----------------|--------------------|-----------------------|---------------------------------|
| -1.27 | -1.80 | -1.54 | 0.53 | Astigmatism 0° |
| 8.01 | 8.25 | 8.12 | -0.24 | Power |
| -1.65 | -1.08 | -1.37 | -0.58 | Astigmatism 45° |
| 0.88 | 0.42 | 0.65 | 0.47 | Trefoil 0° |
| 0.61 | 0.46 | 0.54 | 0.14 | Coma 0° |
| -1.15 | -0.94 | -1.05 | -0.22 | Coma 90° |
| 0.19 | 0.36 | 0.28 | -0.17 | Trefoil 30° |
| -0.77 | -1.15 | -0.96 | 0.38 | Tetrafoil 0° |
| 1.03 | 0.51 | 0.77 | 0.53 | 2 nd Astigmatism 0° |
| 1.42 | 1.49 | 1.46 | -0.07 | Primary Spherical |
| -0.01 | 0.08 | 0.04 | -0.08 | 2 nd Astigmatism 45° |
| 0.08 | -0.02 | 0.03 | 0.10 | Tetrafoil 22.5° |

The most important aberration that is not validated by the 90° rotation test is power. Sources of error that could couple into power are errors measuring absolute distance between the laser tracker and the mirror segment, errors in measuring relative radial changes across the mirror, and axisymmetric angular errors producing surface errors that change as a function of angle of incidence. According to the manufacturer's specifications, the ADM accuracy of the laser tracker is 9.8 $\mu\text{m} + 0.4 \mu\text{m}/\text{m} \approx 20 \mu\text{m}$ of radius error. This uncertainty in distance results in about 35 nm P-V power, so this is negligible. The IFM accuracy of the laser tracker is stated to be 0.4 $\mu\text{m}/\text{m}$. The radial displacement across the mirror surface is only about 0.2 m, so the error in displacement is about 0.1 μm P-V, also negligible. If a conservative assumption is made that there is a rotationally symmetric angular error of 1 μrad at the edge of the mirror, this results in 1.6 μm P-V power or 0.5 μm rms

7. CONCLUSION

A straightforward measurement of an optical surface with a commercial laser tracker at a distance of 22 m is expected to give an accuracy of 5-10 μm rms per sample point. We have made two enhancements to the laser tracker measurements that improve the accuracy by a significant factor. The first is the addition of stability references in the form of distance-measuring interferometers staring at fixed retroreflectors at the edge of the mirror. Part of each reference beam is also reflected to a position sensing detector that measures lateral displacement of the interferometer

beam relative to the mirror. The second improvement is a calibration of the tracker in a geometry that matches the measurement geometry used for testing our mirrors.

With these improvements, the calculations in Table 1 show that the tracker measurements are accurate to better than the 2 μm rms per sample point requirement for guiding the loose-abrasive grinding of GMT. The coefficients of low-order aberrations are measured with an accuracy better than the 0.5 μm rms requirement, limited by spatially correlated errors that are not removed by the stability references and calibration. The enhanced laser tracker system can provide independent measurements of radius of curvature, astigmatism, and other low-order aberrations, at levels within the GMT requirements. When the first optical interferometric measurements are made of the GMT surface, we expect the figure to be accurate enough that interference fringes are easily resolved

Table 2: Laser Tracker Plus system performance. The magnitude and sources of measurement error in the Laser Tracker Plus system that limit the system accuracy are listed on the left. The contributions of these errors to low-order aberrations are listed on the right.

| Laser Tracker Plus System Measurement Accuracy | | | | |
|---|------------------------------|----------------|----------|-------------|
| Category | Source | Direct surface | Angle | Net surface |
| | | microns | microrad | microns |
| Calibration | | | | |
| | distance vs angle | 0.1 | | 0.1 |
| | angle vs angle | | 0.5 | 0.6 |
| Noise | | | | |
| | distance | 0.2 | | 0.2 |
| | angle | | 0.5 | 0.6 |
| Compensation | | | | |
| | distance measurements | 0.1 | | 0.1 |
| | non-linear spatial variation | 0.1 | | 0.1 |
| Net error | | 0.3 | 0.7 | 0.9 |

| Error Contributions to Zernike Polynomials | |
|---|-------------------|
| Aberration | rms surface |
| Power | 0.3 μm |
| Astigmatism | 0.2 μm |
| Coma | 0.1 μm |

8. REFERENCES

- [1] J. H. Burge, L. B. Kot, H. M. Martin, C. Zhao, and T. Zobrist, "Alternative surface measurements for GMT primary mirror segments", in *Optomechanical Technologies for Astronomy*, ed. E. Atad-Ettingui, J. Antebi and D. Lemke, Proc. SPIE **6273** (2006).
- [2] T. Zobrist, J. H. Burge, W. B. Davison, and H. M. Martin, "Measurements of large optical surfaces with a laser tracker", in *Advanced Optical and Mechanical Technologies in Telescopes and Instrumentation*, ed. E. Atad-Ettingui and D. Lemke, Proc. SPIE **7018** (2008).
- [3] H. M. Martin, J. H. Burge, B. Cuerden, W. B. Davison, J. S. Kingsley, W. C. Kittrell, R. D. Lutz, S. M. Miller, C. Zhao, and T. Zobrist, "Progress in manufacturing the first 8.4 m off-axis segment for the Giant Magellan Telescope", in *Advanced Optical and Mechanical Technologies in Telescopes and Instrumentation*, ed. E. Atad-Ettingui and D. Lemke, Proc. SPIE **7018** (2008).
- [4] M. Johns, "Progress on GMT", in *Advanced Optical and Mechanical Technologies in Telescopes and Instrumentation*, ed. E. Atad-Ettingui and D. Lemke, Proc. SPIE **7018** (2008).
- [5] J. H. Burge, W. Davison, C. Zhao, and H. M. Martin, "Development of surface metrology for the Giant Magellan Telescope primary mirror", in *Advanced Optical and Mechanical Technologies in Telescopes and Instrumentation*, ed. E. Atad-Ettingui and D. Lemke, Proc. SPIE **7018** (2008).
- [6] H. M. Martin, J. H. Burge, S. D. Miller, B. K. Smith, R. Zehnder, and C. Zhao, "Manufacture of a 1.7-m prototype of the GMT primary mirror segments", in *Optomechanical Technologies for Astronomy*, ed. E. Atad-Ettingui, J. Antebi and D. Lemke, Proc. SPIE **6273** (2006).
- [7] C. Zhao and J. H. Burge, "Orthonormal vector polynomials in a unit circle, Part I: basis set derived from gradients of Zernike polynomials", *Optics Express*, **15**:18014 (2007).